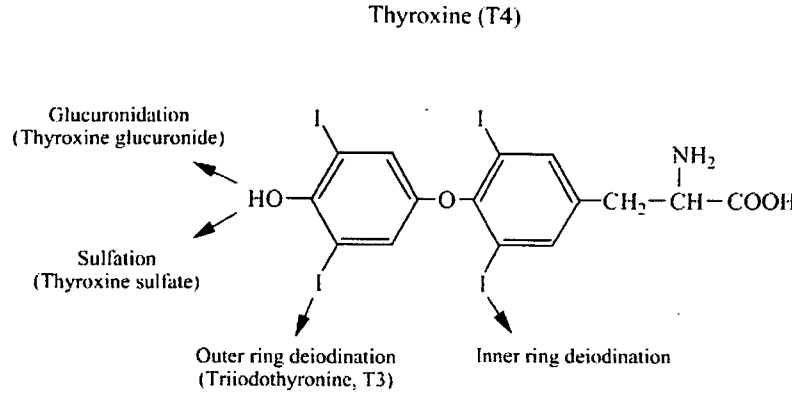


FIG. 1. Major metabolic pathways of thyroxine in human.

TABLE 1

*Tissue distribution of human UGT mRNAs*

Data are from King et al. (2000), Tukey and Strassburg (2000), Fisher et al. (2001), Levesque et al. (2001), Basu et al. (2004), and Finel et al. (2005).

| Tissue | UGT Isoform | | | | | | | | | | | | | | | |
|---|---|---|---|---|---|---|---|---|---|---|---|---|---|---|---|---|
| | 1A1 | 1A3 | 1A4 | 1A5 | 1A6 | 1A7 | 1A8 | 1A9 | 1A10 | 2B4 | 2B7 | 2B10 | 2B11 | 2B15 | 2B17 | 2B28 |
| Liver | + | + | + | + | + | − | − | + | − | + | + | + | + | + | + | + |
| Intestine | + | + | + | + | + | − | + | − | + | + | + | + | − | + | − | + |
| Kidney | − | − | − | N.D. | + | + | − | + | + | + | + | + | + | + | + | + |

N.D., no data: +, present; −, not detectable.

drugs, but extrahepatic tissues also contribute significantly to the glucuronidation of certain drugs in human (Krishna and Klotz, 1994). It is conceivable that the glucuronidation of thyroxine occurs not only in liver but also in intestine and kidney. The second purpose of the present study is to characterize thyroxine glucuronidation in human liver, jejunum, and kidney microsomes, and to identify the UGT isoforms involved in the glucuronidation in each tissue.

## Materials and Methods

**Materials.** Thyroxine, UDP-glucuronic acid (UDPGA), and alamethicin were purchased from Sigma-Aldrich (St. Louis, MO). Bilirubin, chenodeoxycholic acid, serotonin, imipramine hydrochloride, and propofol were purchased from Wako Pure Chemicals (Osaka, Japan). Morphine hydrochloride was from Takeda Chemical Industries (Osaka, Japan). Pooled human liver microsomes (lot H161), microsomes from 12 individual human livers (H003, H023, H030, H043, H056, H064, H066, H070, H089, H093, H112, and HK23), recombinant human UGT1A1, UGT1A3, UGT1A4, UGT1A6, UGT1A7, UGT1A8, UGT1A9, UGT1A10, UGT2B4, UGT2B7, UGT2B15, and UGT2B17 expressed in baculovirus-infected insect cells (Supersomes), and UGT control Supersomes were purchased from BD Gentest (Woburn, MA). The human jejunum (lot HJM0023) or kidney (lot 045290170002) microsomes from an individual donor were purchased from KAC (Kyoto Japan). All other chemicals and solvents were of analytical or the highest grade commercially available.

**Thyroxine Glucuronidation Assay.** A typical incubation mixture (100 μl total volume) contained 100 mM Tris-HCl buffer (pH 7.4), 5 mM $MgCl_2$, 5 mM UDPGA, 25 μg/ml alamethicin, 0.4 mg/ml human liver, jejunum, or kidney microsomes or recombinant UGTs, and 50 μM thyroxine. Thyroxine was dissolved in dimethyl sulfoxide/0.05 M sodium hydroxide (50:50). The final concentration of the organic solvents in the incubation mixture was 1% (v/v). The reaction was initiated by the addition of UDPGA. After incubation at 37°C for 90 min, the reaction was terminated by adding 100 μl of ice-cold 94% acetnitrile/6% formic acid. After the centrifugation at 12,000 rpm for 5 min, the supernatant was filtered with a 0.22-μm filter (Ultrafree-MC centrifugal filter unit; Millipore, Eschborn, Germany). Aliquots of 10 μl were injected into the LC-MS/MS system.

**LC-MS/MS Analysis for Thyroxine Glucuronides.** LC was performed using an HP1100 system including a binary pump, an automatic sampler, and a column oven (Agilent Technologies, Waldbronn, Germany), which was equipped with a Mightysil RP-18 GP (4.6 × 150 mm; 5 μm) column (Kanto Chemical, Tokyo, Japan). The column temperature was 35°C. The mobile phase was 0.1% formic acid (A) and acetonitrile including 0.1% formic acid (B). The conditions for elution were as follows: 25% B (0–1 min); 25 to 70% B (1–4 min); 70% B (4–10 min); 70 to 25% B (10–11 min). Linear gradients were used for all solvent changes. The flow rate was 0.5 ml/min. The LC apparatus was connected to a PE Sciex API2000 tandem mass spectrometer (Applied Biosystems, Langen, Germany) operated in the positive electrospray ionization mode. The turbo gas was maintained at 450°C. Nitrogen was used as the nebulizing, turbo, and curtain gas at 50, 80, and 20 psi, respectively. Parent and/or fragment ions were filtered in the first quadrupole and dissociated in the collision cell using nitrogen as the collision gas. The collision energy was 20 V and 26 V for thyroxine and thyroxine glucuronides, respectively. Two mass/charge (*m/z*) ion transitions were recorded in the multiple reaction monitoring mode: *m/z* 778 and 778 for thyroxine, and *m/z* 954 and 778 for thyroxine glucuronide. The retention times of thyroxine glucuronide and thyroxine were 7.1 min and 8.9 min, respectively. For the quantification of thyroxine glucuronide, the eluate of the HPLC from the incubation mixture including thyroxine glucuronide was collected, referring to the retention time. A part of the eluate was incubated with 800 U/ml β-glucuronidase at 37°C for 24 h. The produced thyroxine was quantified by LC-MS/MS. Once we determined the peak area per known content of thyroxine glucuronide, the ratio was applied to the calculation of the thyroxine glucuronide formed in the incubation mixtures.

**Kinetic Analyses of Thyroxine Glucuronidation in Human Liver, Jejunum, and Kidney Microsomes or Recombinant UGTs.** Thyroxine glucuronosyltransferase activities were determined as described above with substrate concentrations from 2 μM to 100 μM. Kinetic parameters were estimated from the fitted curve using a computer program (KaleidaGraph; Synergy Software, Reading, PA) designed for nonlinear regression analysis. The following equations were applied for Michaelis-Menten kinetics (eq. 1) or substrate inhibition kinetics (eq. 2) (Houston and Kenworthy, 2000):

$$V = V_{max} \times S/(K_m + S) \quad (1)$$

$$V = V_{max} \times S/(K_m + S + S^2/K_{si}) \quad (2)$$

where $V$ is the velocity of the reaction, $S$ is the substrate concentration, $K_m$ is Michaelis-Menten constant, $V_{max}$ is the maximum velocity, and $K_{si}$ is the

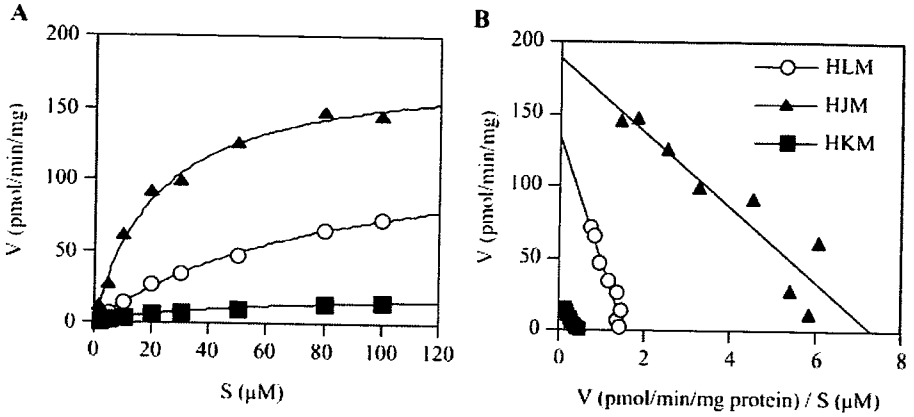


FIG. 2. Kinetic analyses of thyroxine glucuronosyltransferase activities in human liver, jejunum, or kidney microsomes. Michaelis-Menten plots (A) or Eadie-Hofstee plots (B) are shown. Microsomes were incubated with 2 to 100 μM thyroxine and 5 mM UDPGA at 37°C for 90 min. Each data point represents the mean of triplicate determinations. HLM, human liver microsomes; HJM, human jejunum microsomes; HKM, human kidney microsomes.

substrate inhibition constant. Data are expressed as mean ± S.D. of three independent determinations.

**Estimation of Tissue Clearances from in Vitro Data.** In vivo clearance was scaled-up by an equation (Obach et al., 1997; Soars et al., 2002):

$$CL = \frac{V_{max}}{K_m} \times \frac{\text{Microsomal protein}}{\text{Tissue}} (\text{mg/g}) \times \frac{\text{Tissue}}{\text{Body weight}} (\text{g/kg})$$

According to a previous study (Soars et al., 2002), 45, 3, and 45 mg/g tissue were used as the contents of the microsomal protein in liver, intestine, and kidney, respectively. For the weights of liver, intestine, and kidney, 20, 30, and 4.4 g/kg body weight, respectively, were used.

**Immunoblot Analysis of Recombinant Human UGT1A Isoforms.** SDS-polyacrylamide gel electrophoresis and immunoblot analysis of recombinant UGT1A isoforms were performed according to the method of Laemmli (1970). The microsomes from baculovirus-infected insect cells (0.5 μg) were separated on 10% polyacrylamide gel and transferred electrophoretically to a polyvinylidene difluoride membrane Immobilon-P (Millipore, Bedford, MA). Rabbit anti-human UGT1A polyclonal antibodies (BD Gentest) react with all human UGT1A isoforms, since the antibodies recognize the conserved C-terminal region of UGT1A isoforms (Malfatti and Felton, 2004). Biotinylated anti-rabbit IgG and a VECTASTAIN ABC kit (Vector Laboratories, Burlingame, CA) were used for diaminobenzidine staining. The densities of the bands were determined using an ImageQuant (GE Healthcare Bio-Sciences Corp., Piscataway, NJ). For each isoform, the densities of multiple bands, possibly owing to variability in glycosylation (Malfatti and Felton, 2004), were summed for the quantification. The expression level of UGT1A was defined based on a standard curve using recombinant UGT1A1 (1 unit per 1 mg protein).

**Other Glucuronidation Assays.** Bilirubin *O*-glucuronosyltransferase (Katoh et al., 2007), imipramine *N*-glucuronosyltransferase (Nakajima et al., 2002), and serotonin *O*-glucuronosyltransferase (Fujiwara et al., 2007) activities in microsomes from 12 human livers were determined according to methods established in our laboratory. Chenodeoxycholic acid 24-*O*-glucuronosyltransferase activities in these human liver microsomes were determined according to the method of Trottier et al. (2006) with slight modifications. Estradiol 3-*O*-, propofol *O*-, and morphine 3-*O*-glucuronosyltransferase activities in these human liver microsomes were provided by the manufacturer.

**Correlation Analyses.** Correlation between thyroxine glucuronidation and the other glucuronosyltransferase activities was determined by unpaired Student's *t* test. A *p* value of less than 0.05 was considered statistically significant.

**Inhibition Analysis of Thyroxine Glucuronosyltransferase Activities in Human Liver, Jejunum, and Kidney Microsomes or Recombinant UGTs.** Bilirubin is a typical substrate of UGT1A1 (King et al., 2000). Imipramine is a substrate of UGT1A3 and UGT1A4 (Green and Tephly, 1998). Emodin is a substrate of UGT1A1, UGT1A3, UGT1A8, and UGT1A9 (King et al., 2000). Propofol is a substrate of UGT1A8 and UGT1A9 (King et al., 2000). Troglitazone is a substrate of UGT1A1, UGT1A8, and UGT1A10 (Watanabe et al., 2002). Bilirubin was dissolved in 0.1 M sodium hydroxide. Imipramine hydrochloride was dissolved in water. Emodin and troglitazone were dissolved in dimethyl sulfoxide. Propofol was dissolved in methanol. These compounds were added to the incubation mixtures described above to investigate their inhibitory effects on the thyroxine glucuronosyltransferase activities in human liver, jejunum, and kidney microsomes or recombinant UGTs. The final concentration of the organic solvents in the incubation mixture was <2% (v/v). The substrate concentration was 20 μM.

## Results

**Thyroxine Glucuronosyltransferase Activities in Human Liver, Jejunum, or Kidney Microsomes.** The formation of thyroxine glucuronide increased in a microsomal protein concentration- and time-dependent manner. The formations were linear at least for 0.5 mg/ml microsomal protein and 120 min incubation (data not shown). Unless specified, the typical incubation mixture containing 0.4 mg/ml microsomal protein was incubated at 37°C for 90 min. The kinetics of thyroxine glucuronosyltransferase activities in human liver, jejunum, and kidney microsomes were fitted to the Michaelis-Menten equation (Fig. 2A). The Eadie-Hofstee plots were monophasic (Fig. 2B). The apparent $K_m$ and $V_{max}$ values are summarized in Table 2. Human jejunum microsomes showed a lower $K_m$ value (24.2 μM) than did human liver (85.9 μM) and kidney (53.3 μM) microsomes. Human kidney microsomes showed a lower $V_{max}$ (22.6 pmol/min/mg) value than did human liver (133.4 pmol/min/mg) and jejunum (184.6 pmol/min/mg) microsomes. The in vitro intrinsic clearances ($V_{max}/K_m$) of thyroxine glucuronidation in human liver, jejunum, and kidney microsomes were 1.6, 7.8, and 0.4 μl/min/mg, respectively. By scaling-up, the in vivo clearances in liver, intestine, and kidney were estimated to be 1440, 702, and 79 μl/min/kg body weight, respectively.

**Thyroxine Glucuronosyltransferase Activities by Recombinant UGT Isoforms.** Eleven recombinant UGT isoforms expressed in baculovirus-infected insect cells were used to determine their thyroxine glucuronosyltransferase activities. As shown in Fig. 3A, UGT1A8 exhibited the highest thyroxine glucuronosyltransferase activity (87 pmol/min/mg), followed by UGT1A1 (26 pmol/min/mg), UGT1A10 (20 pmol/min/mg), UGT1A3 (18 pmol/min/mg), UGT1A9 (5 pmol/min/mg), and UGT1A7 (5 pmol/min/mg). To quantify the expression level of UGT1A in each expression system, immunoblot analysis was performed (Fig. 3B). In accordance with previous studies (Malfatti and Felton, 2004; Fujiwara et al., 2007), the recombinant UGT1A isoforms showed multiple bands, possibly owing to variability in the glycosylation. Based on a UGT1A1 level of 1.00 unit/mg, the expression levels of the other isoforms were determined as follows: UGT1A3, 0.20 unit/mg; UGT1A4, 0.38 unit/mg; UGT1A6, 0.95 unit/mg; UGT1A7, 0.60 unit/mg; UGT1A8, 0.80 unit/mg; UGT1A9, 0.68 unit/mg; and UGT1A10, 0.42 unit/mg. By normalization with the UGT expression levels (Fig. 3C), UGT1A8 (108.7 pmol/min/unit) and UGT1A3 (91.6 pmol/min/unit) exhibited the highest thyroxine glucuronosyltransferase activities, followed by UGT1A10 (47.3 pmol/

TABLE 2

*Kinetic parameters of thyroxine glucuronosyltransferase activities in human liver, jejunum, and kidney microsomes, and by recombinant UGTs*

| Enzyme | $K_m$ | $V_{max}$ | | | $V_{max}/K_m$ |
|---|---|---|---|---|---|
| | *μM* | *pmol/min/mg* | | | *μl/min/mg* |
| HLM | 85.9 ± 6.9 | 133.4 ± 9.8 | | | 1.6 ± 0.0 |
| HJM | 24.2 ± 4.1 | 184.6 ± 7.0 | | | 7.8 ± 1.0 |
| HKM | 53.3 ± 5.4 | 22.6 ± 1.8 | | | 0.4 ± 0.0 |
| | $K_m$ | $V_{max}$ | Corrected $V_{max}$ | $K_{si}$ | Corrected $V_{max}/K_m$ |
| | *μM* | *pmol/min/mg* | *pmol/min/unit* | *μM* | *μl/min/unit* |
| UGT1A1 | 104.9 ± 6.6 | 75.7 ± 0.7 | 75.7 ± 0.7 | | 0.7 ± 0.1 |
| UGT1A3 | 33.2 ± 2.2 | 40.8 ± 2.4 | 204.0 ± 11.9 | 83.5 ± 14.3 | 6.2 ± 0.1 |
| UGT1A7 | 38.1 ± 2.5 | 8.2 ± 0.3 | 13.7 ± 0.4 | | 0.4 ± 0.0 |
| UGT1A8 | 45.4 ± 8.4 | 239.9 ± 38.2 | 299.9 ± 47.8 | 56.4 ± 22.5 | 6.6 ± 0.2 |
| UGT1A9 | 24.1 ± 1.2 | 7.1 ± 0.9 | 10.4 ± 1.4 | | 0.4 ± 0.0 |
| UGT1A10 | 96.3 ± 27.3 | 146.7 ± 26.3 | 349.4 ± 62.6 | 9.0 ± 1.5 | 3.7 ± 0.4 |

HLM, human liver microsomes; HJM, human jejunum microsomes; HKM, human kidney microsomes
Data are mean ± S.D. of three independent experiments.

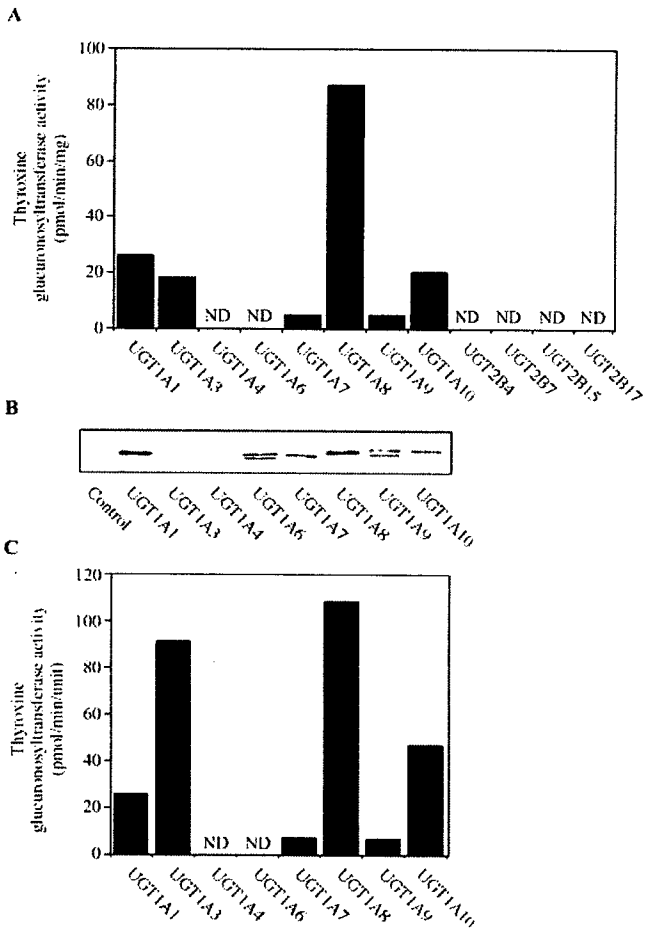


FIG. 3. Thyroxine glucuronosyltransferase activities by recombinant human UGTs expressed in baculovirus-infected insect cells. The substrate concentration was 50 μM. Each column represents the mean of duplicate determinations. The activities are expressed as pmol/min/mg (A) or pmol/min/unit (C) normalized with the UGT1A expression levels determined by immunoblot analysis (B). Immunoblot analysis of the recombinant UGT1A isoforms (0.5 μg) was performed using rabbit anti-human UGT1A antibodies. Control represents the UGT control Supersomes (0.5 μg). The expression levels were defined assuming that UGT1A1 was 1.00 unit/mg. ND, not detected.

min/unit) and UGT1A1 (26.0 pmol/min/unit). The activities by UGT1A7 (7.6 pmol/min/unit) and UGT1A9 (7.1 pmol/min/unit) were low.

**Kinetics of Thyroxine Glucuronosyltransferase Activities by Recombinant UGT1A Isoforms.** For six UGT isoforms showing thyroxine glucuronosyltransferase activity, kinetic analyses were performed. The kinetics of thyroxine glucuronosyltransferase activities by recombinant UGT1A1, UGT1A7, and UGT1A9 fitted to the Michaelis-Menten kinetics (Fig. 4A). The activities by recombinant UGT1A3, UGT1A8, and UGT1A10 fitted to the substrate inhibition kinetics (Fig. 4B). The apparent $K_m$ and corrected $V_{max}$ values are summarized in Table 2. The $K_m$ values varied from 24.1 μM to 104.9 μM. UGT1A8 (6.6 μl/min/unit) exhibited the highest clearance, followed by UGT1A3 (6.2 μl/min/unit) and by UGT1A10 (3.7 μl/min/unit). UGT1A1 (0.7 μl/min/unit), UGT1A9 (0.4 μl/min/unit), and UGT1A7 (0.4 μl/min/unit) exhibited low intrinsic clearance.

**Interindividual Variability of Thyroxine Glucuronosyltransferase Activities in Microsomes from 12 Human Livers and Correlation Analyses.** The thyroxine glucuronosyltransferase activity in microsomes from 12 human livers ranged from 23.7 to 84.8 pmol/min/mg protein, representing 3.6-fold variability. Correlation analyses were performed between the thyroxine glucuronosyltransferase activity and typical activities including bilirubin *O*-glucuronidation catalyzed by UGT1A1, estradiol 3-*O*-glucuronidation catalyzed by UGT1A1 and UGT1A8 (Lepine et al., 2004), chenodeoxycholic acid 24-*O*-glucuronidation catalyzed by UGT1A3 (Trottier et al., 2006), imipramine *N*-glucuronidation catalyzed by UGT1A3 and UGT1A4, serotonin *O*-glucuronidation catalyzed by UGT1A6, propofol *O*-glucuronidation catalyzed by UGT1A8 and UGT1A9, or morphine 3-*O*-glucuronidation catalyzed by UGT2B7 (Table 3). Since UGT1A8 is not expressed in human liver, the estradiol 3-*O*- and propofol *O*-glucuronosyltransferase activities represented are the UGT1A1 and UGT1A9 activities, respectively. The thyroxine glucuronosyltransferase activities in 12 human liver microsomes were significantly correlated with bilirubin ($r = 0.855$, $p < 0.001$), estradiol ($r = 0.827$, $p < 0.0001$), and serotonin ($r = 0.522$, $p < 0.05$) glucuronidation.

**Inhibitory Effects of Typical Substrates for UGT Isoforms on Thyroxine Glucuronosyltransferase Activities in Human Liver, Jejunum, and Kidney Microsomes or Recombinant UGTs.** The inhibitory effects of bilirubin, imipramine, emodin, propofol, and troglitazone on thyroxine glucuronosyltransferase activity were investigated. These inhibitors were used at effective concentrations according to previous studies (Watanabe et al., 2002; Kuehl et al., 2005; Yamanaka et al., 2005). The thyroxine glucuronosyltransferase activity in human liver microsomes was strongly inhibited by bilirubin (29% of control) and emodin (15% of control), and was moderately inhibited by troglitazone (51% of control), but was activated by

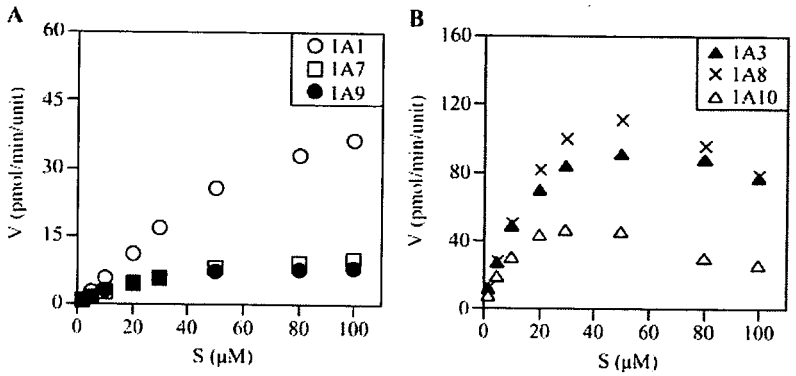


FIG. 4. Kinetic analyses of thyroxine glucuronosyltransferase activities by recombinant UGT1A1, UGT1A3, UGT1A7, UGT1A8, UGT1A9, and UGT1A10. Recombinant UGT1As were incubated with 2 to 100 μM thyroxine and 5 mM UDPGA at 37°C for 90 min. The activities by recombinant UGT1A1, UGT1A7, and UGT1A9 fitted to the Michaelis-Menten kinetics (A). The activities by recombinant UGT1A3, UGT1A8, and UGT1A10 fitted to the substrate inhibition kinetics (B). Each data point represents the mean of triplicate determinations.

TABLE 3

*Correlation coefficients between thyroxine glucuronidation and other glucuronidations in microsomes from 12 human livers*

| Activity (Isoform) | Substrate Concentration | $r$ | $p$ |
|---|---|---|---|
| | μM | | |
| Bilirubin *O*-glucuronidation (UGT1A1) | 10 | 0.855 | <0.001 |
| Estradiol 3-*O*-glucuronidation (UGT1A1) | 100 | 0.827 | <0.0001 |
| Chenodeoxycholic acid 24-*O*-glucuronidation (UGT1A3) | 10 | −0.080 | N.S. |
| Imipramine *N*-glucuronidation (UGT1A3 and UGT1A4) | 500 | 0.135 | N.S. |
| Serotonin *O*-glucuronidation (UGT1A6) | 1000 | 0.522 | <0.05 |
| Propofol *O*-glucuronidation (UGT1A9) | 30 | 0.330 | N.S. |
| Morphine 3-*O*-glucuronidation (UGT2B7) | 250 | −0.035 | N.S. |

N.S., not significant.

propofol (121% of control) (Fig. 5A). The thyroxine glucuronosyltransferase activity in human jejunum microsomes was strongly inhibited by emodin (45% of control) and was moderately inhibited by bilirubin (68% of control). The thyroxine glucuronosyltransferase activity in human kidney microsomes was strongly inhibited by troglitazone (46% of control), and was moderately inhibited by emodin (55% of control). Thus, the effects of these compounds on the activity were different between the tissues. The inhibitory effects on thyroxine glucuronidation were also investigated for recombinant UGT1A isoforms (Fig. 5B). Bilirubin strongly inhibited the activity by UGT1A1 (16% of control) and moderately inhibited the activities by UGT1A7 (68% of control). Imipramine moderately inhibited the activity by UGT1A3 (68% of control) and UGT1A10 (64% of control). Emodin strongly inhibited the activities by all UGT1A isoforms. Propofol moderately inhibited the activities by UGT1A9 (63% of control) and UGT1A10 (66% of control), and activated the activities by UGT1A1 (349% of control) and UGT1A3 (324% of control). Troglitazone strongly inhibited the activities by the five UGT1A isoforms other than UGT1A3.

## Discussion

In this study, we extensively investigated thyroxine glucuronidation in human liver, jejunum, and kidney microsomes and recombinant UGTs. The tissue clearances in liver, intestine, and kidney were estimated to be 1440, 702, and 79 μl/min/kg body weight, respectively. Although the UGT activities are not the same in the region of intestine (Strassburg et al., 2000), it was first demonstrated that intestine exhibited approximately one half the clearance of liver for thyroxine glucuronidation. The glucuronidation in intestine may affect the enterohepatic circulation of thyroxine. In kidney, thyroxine is highly converted to T3 with $K_m$ = 3.0 μM, $V_{max}$ = 26.1 pmol/min/mg, and $V_{max}$/Km = 8.7 μl/min/mg (Boye, 1986). In addition to the outer ring deiodination, this study demonstrated that thyroxine is glucuronidated in kidney.

This is the first study demonstrating that human UGT1A8, UGT1A10, and UGT1A3 have high, and UGT1A1 has moderate catalytic activity toward thyroxine glucuronidation. Since UGT isoforms are expressed differently in human liver, jejunum, and kidney, it was conceivable that UGT isoform(s) responsible for the thyroxine glucuronidation might be different between these tissues. If the absolute protein levels of each UGT isoform in human tissues are available, quantitative estimation of the contribution of each isoform to the concerned activity can be accomplished as for cytochrome P450 (Becquemont et al., 1998). Unfortunately, for UGT, a methodology of quantification is lacking. In addition, specific antibodies against each UGT1A isoform are limited. In the present study, we qualitatively identified the UGT isoforms that are responsible for the thyroxine glucuronidation in human tissues by kinetic, correlation, and inhibition analyses as well as tissue distribution of each UGT isoform.

The Eadie-Hofstee plots of thyroxine glucuronosyltransferase activities in human liver, jejunum, and kidney microsomes were monophasic, suggesting that one or more UGT isoforms would be involved in the activities. In human liver microsomes, the apparent $K_m$ value was similar to that of recombinant UGT1A1. The activity in a panel of human liver microsomes was significantly correlated with the bilirubin *O*- and estradiol 3-*O*-glucuronosyltransferase activities catalyzed by UGT1A1. Although the thyroxine glucuronosyltransferase activity was also correlated with the serotonin *O*-glucuronosyltransferase activity catalyzed by UGT1A6, it might be a fortuitous result, because the serotonin *O*-glucuronosyltransferase activity was significantly ($r$ = 0.627, $p$ < 0.005) correlated with the estradiol 3-*O*-glucuronosyltransferase activity in the panel of human liver microsomes. These results suggested that a major UGT isoform responsible for the thyroxine glucuronidation in human liver microsomes would be UGT1A1. We could not exclude the possibility that UGT1A9 might also contribute to the thyroxine glucuronosyltransferase activity in human liver microsomes. Interestingly, propofol activated the thyroxine glucuronosyltransferase activity in human liver microsomes. It has been reported that propofol activated 4-methylunbelliferone glucuronidation by recombinant UGT1A1 (Mano et al., 2004). Thus, the result supported the finding that a major isoform responsible for thyroxine glucuronidation in human liver microsomes would be UGT1A1. We used propofol as an inhibitor of UGT1A8 and UGT1A9. However, our previous study found that propofol can activate *trans*-3′-hydroxicotinine *O*-glucuronidation by recombinant UGT1A9 (Yamanaka et al., 2005). Propofol might not be an

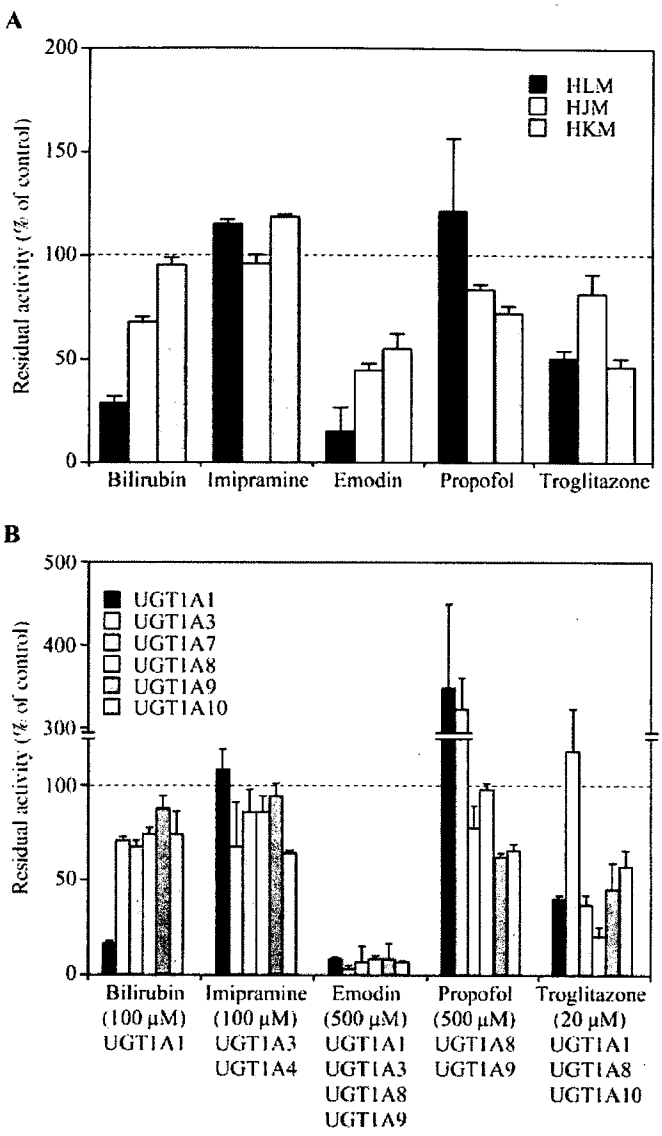


FIG. 5. Effects of typical substrates for UGTs on thyroxine glucuronosyltransferase activities in human liver, jejunum, and kidney microsomes (A) or recombinant UGTs (B). Bilirubin (UGT1A1), imipramine (UGT1A3 and UGT1A4), emodin (UGT1A1, UGT1A3, UGT1A8, and UGT1A9), propofol (UGT1A8 and UGT1A9), and troglitazone (UGT1A1, UGT1A8, and UGT1A10) were used as inhibitors. A, control activities in human liver microsomes (HLM), human jejunum microsomes (HJM), and human kidney microsomes (HKM) at 20 μM thyroxine were 26.7 pmol/min/mg, 90.9 pmol/min/mg, and 6.2 pmol/min/mg, respectively. B, control activities for 20 μM thyroxine by recombinant UGT1A1, UGT1A3, UGT1A7, UGT1A8, UGT1A9, and UGT1A10 were 11.1 pmol/min/unit, 69.2 pmol/min/unit, 4.7 pmol/min/unit, 81.5 pmol/min/unit, 4.7 pmol/min/unit, and 42.6 pmol/min/unit, respectively. Each data point represents the mean ± S.D. of triplicate determinations.

appropriate inhibitor. The contribution of UGT1A3 to the thyroxine glucuronidation in human liver microsomes would be negligible, because the thyroxine glucuronosyltransferase activity in the panel of human liver microsomes was not correlated with the chenodeoxycholic acid 24-*O*-glucuronosyltransferase activity catalyzed by UGT1A3 (Table 3), and imipramine did not inhibit the thyroxine glucuronosyltransferase activity (Fig. 5) although it inhibited the chenodeoxycholic acid 24-*O*-glucuronosyltransferase activity by 48% of control (data not shown).

In human jejunum microsomes, the apparent $K_m$ value was similar to that of recombinant UGT1A8. The thyroxine glucuronidation in human jejunum microsomes was inhibited by emodin, and was moderately inhibited by bilirubin. These results suggested that the thyroxine glucuronidation in human jejunum microsomes might be catalyzed mainly by UGT1A8 and UGT1A10, and to a minor extent by UGT1A1. In human kidney microsomes, the apparent $K_m$ value was similar to that of recombinant UGT1A7. The thyroxine glucuronidation in human kidney microsomes was inhibited by troglitazone and emodin. It was suggested that the thyroxine glucuronidation in human kidney microsomes might be catalyzed by UGT1A7, UGT1A9, and UGT1A10. In summary, the contribution of each UGT1A isoform would vary between human tissues, depending on the relative abundance of each isoform.

In conclusion, we characterized the thyroxine glucuronidation in human liver, intestine, and kidney microsomes and found that UGT1A1 in the liver, UGT1A8 and UGT1A10 in the intestine, and UGT1A7, UGT1A9, and UGT1A10 in the kidney mainly contribute to the activity. The change of activities of these UGTs via inhibition and induction by administered drugs (Kiang et al., 2005) as well as genetic polymorphisms (Miners et al., 2002) may be a causal factor of interindividual differences in the plasma thyroxine concentration.

**Acknowledgments.** We acknowledge Brent Bell for reviewing the manuscript.

## References

Basu NK, Ciotti M, Hwang MS, Kole L, Mitra PS, Cho JW, and Owens IS (2004) Differential and special properties of major human *UGT1*-encoded gastrointestinal UDP-glucuronosyltransferases enhance potential to control chemical uptake. *J Biol Chem* **279**:1429–1441.

Becquemont L, Le Bot MA, Riche C, Funck-Brentano C, Jaillon P, and Beaune P (1998) Use of heterologously expressed human cytochrome P450 1A2 to predict tacrine-fluvoxamine drug interaction in man. *Pharmacogenetics* **8**:101–108.

Boye N (1986) Thyroxine monodeiodination in normal human kidney tissue in vitro. *Acta Endocrinol* **112**:536–540.

Findlay KAB, Kaptein E, Visser TJ, and Burchell B (2000) Characterization of the uridine diphosphate-glucuronosyltransferase-catalyzing thyroid hormone glucuronidation in man. *J Clin Endocrinol Metab* **85**:2879–2883.

Finel M, Li X, Gardner-Stephen D, Bratton S, Mackenzie PI, and Radominska-Pandya A (2005) Human UDP-glucuronosyltransferase 1A5: identification, expression, and activity. *J Pharmacol Exp Ther* **315**:1143–1149.

Fisher MB, Paine MF, Strelevitz TJ, and Wrighton SA (2001) The role of hepatic and extrahepatic UDP-glucuronosyltransferases in human drug metabolism. *Drug Metab Rev* **33**:273–297.

Fujiwara R, Nakajima M, Yamanaka H, Nakamura A, Katoh M, Ikushiro S, Sakaki T, and Yokoi T (2007) Effects of coexpression of UGT1A9 on enzymatic activities of human UGT1A isoforms. *Drug Metab Dispos* **35**:747–757.

Green MD and Tephly TR (1998) Glucuronidation of amine substrates by purified and expressed UDP-glucuronosyltransferase proteins. *Drug Metab Dispos* **26**:860–867.

Houston JB and Kenworthy K (2000) In vitro-in vivo scaling of CYP kinetic data not consistent with the classical Michaelis-Menten model. *Drug Metab Dispos*, **28**:246–254.

Hulbert AJ (2000) Thyroid hormones and their effects: a new perspective. *Biol Rev Camb Philos Soc* **75**:519–631.

Isojarvi JI, Pakarinen AJ, and Myllyla VV (1992) Thyroid function with antiepileptic drugs. *Epilepsia* **33**:142–148.

Katoh M, Matsui T, and Yokoi T (2007) Glucuronidation of antiallergic drug, tranilast: identification of human UGT isoforms and effect of its phase I metabolite. *Drug Metab Dispos*, **35**:583–589.

Kiang TK, Ensom MH, and Chang TK (2005) UDP-glucuronosyltransferases and clinical drug-drug interactions. *Pharmacol Ther* **106**:97–132.

King CD, Rios GR, Green MD, and Tephly TR (2000) UDP-glucuronosyltransferases. *Curr Drug Metab* **1**:143–161.

Krishna DR and Klotz U (1994) Extrahepatic metabolism of drugs in humans. *Clin Pharmacokinet* **26**:144–160.

Kuehl GE, Lampe JW, Potter JD, and Bigler J (2005) Glucuronidation of nonsteroidal anti-inflammatory drugs: identifying the enzymes responsible in human liver microsomes. *Drug Metab Dispos* **33**:1027–1035.

Laemmli UK (1970) Cleavage of structural proteins during the assembly of the head of bacteriophage T4. *Nature* **227**:680–685.

Leonard JL and Koehrle J (1996) Interacellular pathways of iodothyronine metabolism, in *Werner and Ingbar's The Thyroid, A Fundamental and Clinical Text*, 7th ed (Braverman LE and Utiger RD eds) pp 125–161. Lippincott-Raven, Philadelphia.

Lepine J, Bernard O, Plante M, Tetu B, Pelletier G, Labrie F, Belanger A, and Guillemette C (2004) Specificity and regioselectivity of the conjugation of estradiol, estrone, and their catecholestrogen and methoxyestrogen metabolites by human uridine diphosphoglucuronosyltransferases expressed in endometrium. *J Clin Endocrinol Metab* **89**:5222–5232.

Levesque E, Turgeon D, Carrier JS, Montminy V, Beaulieu M, and Belanger A (2001) Isolation and characterization of the UGT2B28 cDNA encoding a novel human steroid conjugating UDP-glucuronosyltransferase. *Biochemistry* **40**:3869–3881.

Mackenzie PI, Walter Bock K, Burchell B, Guillemette C, Ikushiro S, Iyanagi T, Miners JO, Owens IS, and Nebert DW (2005) Nomenclature update for the mammalian UDP glycosyltransferase (UGT) gene superfamily. *Pharmacogenet Genomics* **15**:677–685.

Malfatti MA and Felton JS (2004) Human UDP-glucuronosyltransferase 1A1 is the primary

enzyme responsible for the *N*-glucuronidation of *N*-hydroxy-PhIP in vitro. *Chem Res Toxicol* **17**:1137–1144.
Mano Y, Usui T, and Kamimura H (2004) In vitro inhibition and stimulation of β-estradiol and propofol on the 4-methylumbelliferone glucuronidation by recombinant human UGT isozymes 1A1, 1A8 and 1A9. *Biopharm Drug Dispos* **25**:339–344.
Miners JO, McKinnon RA, and Mackenzie PI (2002) Genetic polymorphisms of UDP-glucuronosyltransferases and their functional significance. *Toxicology* **181–182**:453–456.
Nakajima M, Tanaka E, Kobayashi T, Ohashi N, Kume T, and Yokoi T (2002) Imipramine *N*-glucuronidation in human liver microsomes: biphasic kinetics and characterization of UGT isoforms. *Drug Metab Dispos* **30**:636–642.
Obach RS, Baxter JG, Liston TE, Silber BM, Jones BC, MacIntyre F, Rance DJ, and Wastall P (1997) The prediction of human pharmacokinetic parameters from preclinical and in vitro metabolism data. *J Pharmacol Exp Ther* **283**:46–58.
Ohnhaus EE and Studer H (1983) A link between liver microsomal enzyme activity and thyroid hormone metabolism in man. *Br J Clin Pharmacol* **15**:71–76.
Soars MG, Burchell B, and Riley RJ (2002) In vitro analysis of human drug glucuronidation and prediction of in vivo metabolic clearance. *J Pharmacol Exp Ther* **301**:382–390.
Strassburg CP, Kneip S, Topp J, Obermayer-Straub P, Barut A, Tukey RH, and Manns MP (2000) Polymorphic gene regulation and interindividual variation of UDP-glucuronosyltransferase activity in human small intestine. *J Biol Chem* **275**:36164–36171.
Trottier J, Verreault M, Grepper S, Monte D, Belanger J, Kaeding J, Caron P, Inaba T, and Barbier O (2006) Human UDP-glucuronosyltransferase (UGT) 1A3 enzyme conjugates chenodeoxycholic acid in the liver. *Hepatology* **44**:1158–1170.
Tukey RH and Strassburg CP (2000) Human UDP-glucuronosyltransferase: metabolism, expression, and disease. *Annu Rev Pharmacol Toxicol* **40**:581–616.
Visser TJ (1994) Sulfation and glucuronidation pathways of thyroid hormone metabolism, in *Thyroid Hormone Metabolism: Molecular Biology and Alternate Pathways* (Wu SY and Visser TJ eds) pp 85–117. CRC Press, Boca Raton, FL.
Watanabe Y, Nakajima M, and Yokoi T (2002) Troglitazone glucuronidation in human liver and intestine microsomes: high catalytic activity of UGT1A8 and UGT1A10. *Drug Metab Dispos* **30**:1462–1469.
Wu Y and Koenig RJ (2000) Gene regulation by thyroid hormone. *Trends Endocrinol Metab* **11**:207–211.
Yamanaka H, Nakajima M, Katoh M, Kanoh A, Tamura O, Ishibashi H, and Yokoi T (2005) *trans*-3′-Hydroxycotinine *O*- and *N*-glucuronidations in human liver microsomes. *Drug Metab Dispos* **33**:23–30.
Zhang J and Lazar MA (2000) The mechanism of action of thyroid hormones. *Annu Rev Physiol* **62**:439–466.

**Address correspondence to:** Dr. Tsuyoshi Yokoi, Drug Metabolism and Toxicology, Division of Pharmaceutical Sciences, Graduate School of Medical Science, Kanazawa University, Kakuma-machi, Kanazawa 920-1192, Japan. E-mail: tyokoi@kenroku.kanazawa-u.ac.jp

# Post-transcriptional regulation of human pregnane X receptor by microRNA affects the expression of cytochrome P450 3A4

Shingo Takagi, Miki Nakajima, Takuya Mohri & Tsuyoshi Yokoi

Drug Metabolism and Toxicology, Division of Pharmaceutical Sciences, Graduate School of Medical Science, Kanazawa University, Kakuma-machi, Kanazawa 920-1192, Japan.

E-mail
Shingo Takagi: forscher@p.kanazawa-u.ac.jp
Miki Nakajima: nmiki@kenroku.kanazawa-u.ac.jp
Takuya Mohri: shigemou@stu.kanazawa-u.ac.jp
Tsuyoshi Yokoi: tyokoi@kenroku.kanazawa-u.ac.jp

To whom all correspondence should be addressed:
Tsuyoshi Yokoi, Ph.D.
Drug Metabolism and Toxicology
Division of Pharmaceutical Sciences
Graduate School of Medical Science
Kanazawa University
Kakuma-machi
Kanazawa 920-1192, Japan
Tel / Fax +81-76-234-4407
E-mail: tyokoi@kenroku.kanazawa-u.ac.jp

Running title: microRNA regulates human PXR

## SUMMARY

Pregnane X receptor (PXR) is a major transcription factor regulating the inducible expression of a variety of transporters and drug-metabolizing enzymes including cytochrome P450 (CYP) 3A4. We first found that the PXR mRNA level was not correlated with the PXR protein level in a panel of 25 human livers, indicating the involvement of post-transcriptional regulation. Notably, a potential miR-148a recognition element was identified in the 3' untranslated region of human PXR mRNA. We investigated whether PXR might be regulated by miR-148a. Reporter assay revealed that miR-148a could recognize the miR-148a recognition element of PXR mRNA. The PXR protein level was decreased by the overexpression of miR-148a, while it was increased by inhibition of miR-148a. The miR-148a-dependent decrease of PXR protein attenuated the induction CYP3A4 mRNA. Furthermore, the translational efficiency of PXR (PXR protein/PXR mRNA ratio) was inversely correlated with the expression levels of miR-148a in a panel of 25 human livers, supporting the miR-148a-dependent regulation of PXR in human livers. Eventually, the PXR protein level was significantly correlated with the CYP3A4 mRNA and protein levels. In conclusion, we found that miR-148a post-transcriptionally regulated human PXR, resulting in the modulation of the inducible and/or constitutive levels of CYP3A4 in human liver. This study will provide new insight into the unsolved mechanism of the large interindividual variability of CYP3A4 expression.

## INTRODUCTION

A key function of the liver is the metabolism and elimination of xenobiotics or endobiotics. The expression of genes involved in these processes is largely regulated by transcription factors belonging to the nuclear receptor family. Pregnane X receptor (PXR; alternate names SXR, PAR, NR1I2), a member of the nuclear receptor family, is a crucial regulator of drug metabolism and elimination. It is predominantly expressed in liver and small intestine. PXR is activated by a broad spectrum of xenobiotics including antibiotics, antimycotics, and herbal components (1), dimerizes with retinoid X receptor α (RXRα) and binds to response elements of target genes including cytochrome P450s (CYPs), UDP-glucuronosyltransferases (UGTs), glutathione *S*-transferases (GSTs), sulfotransferases (SULTs), and various transporters such as multidrug resistance 1 (MDR1) and multidrug resistance associated protein 2 (MRP-2) to induce them (2). Thus, PXR is recognized as a xenosensor for the detoxification of foreign compounds. However, it also plays a role as a physiological sensor of bile acids to protect the body from toxicity by regulating the expression of target genes that decreases the synthesis and increases the elimination of bile acids (3, 4).

One of the best-known genes regulated by PXR is CYP3A4, the most abundant P450 in human liver that catalyze the metabolism of over 50% of current prescription drugs (5-7). A large interindividual difference (~50-fold) has been reported for the CYP3A4 level in the general population (8), which cannot be explained by genetic polymorphisms (9, 10). The CYP3A4 expression is largely regulated at the transcriptional level by transcriptional factors such as CCAAT/enhancer-binding proteins, C/EBPα and C/EBPβ and hepatocyte nuclear factors, HNF4α and HNF3γ as well as constitutive androstane receptor (CAR) and PXR (11). However, the cause of the large interindividual variability in CYP3A4 level is poorly understood, and is an urgent issue to be solved. The regulation by PXR may, in part, be responsible for such variability since PXR is activated by endogenous compounds such as steroid hormones and bile acids (1, 12),

PXR regulates many targets controlling pharmacokinetics, but its own regulation is not fully understood, with reports showing only that human PXR is induced by dexamethasone through glucocorticoid receptor (13) or by clofibrate through peroxisome proliferators-activated receptor α (14). Employing an on-line search using the miRBase Target database (15, http://microrna.sanger.ac.uk/), we found some potential recognition sites for microRNAs (miRNAs) in the 3' untranslated region (UTR) of the human PXR.

miRNAs are a recently discovered family of short non-coding RNA whose final product is an approximately 22 nucleotide functional RNA molecule (16). They play important roles in the regulation of target genes by binding to complementary regions of transcripts to repress

their translation or regulate degradation. At present, more than 400 miRNAs have been identified in humans and miRNAs are predicted to control about 30% of the genes within the human genome (17, 18). The roles of miRNAs have received attention especially in the cancer field, but hardly yet in the field of pharmacokinetics. In the present study, we investigated whether human PXR might be post-transcriptionally regulated by miRNA and its impact on the CYP3A4 expression.

## EXPERIMENTAL PROCEDURES

*Chemicals and reagents* - Rifampicin was obtained from Wako Pure Chemicals (Osaka, Japan). The pGL3-promoter vector, pGL4.74-TK plasmid, Tfx-20 reagent and dual-luciferase reporter assay system were purchased from Promega (Madison, WI). Lipofectamine 2000, Lipofectamine RNAiMAX were from Invitrogen (Carlsbad, CA). Pre-miR miRNA Precursors for miR-148a and for the negative control were from Ambion (Austin, TX). Locked nucleic acid (LNA) modified antisense oligonucleotides (AsOs) for miR-148a (5'-ACAAAGTTCTGTAGTGCACTGA-3', LNA is indicated by underline) and for the negative control (5'-AGACUAGCGGUAUCUUAAACC-3') were commercially synthesized at Greiner Bio-One (Tokyo, Japan). All primers and oligonucleotides were commercially synthesized at Hokkaido System Sciences (Sapporo, Japan). Goat anti-human PXR polyclonal antibodies (N-16), rabbit anti-human RXRα polyclonal antibodies (D-20), and goat anti-human HNF4α polyclonal antibodies (S-20) were from Santa Cruz Biotechnology (Santa Cruz, CA). Rabbit anti-CYP3A4 polyclonal antibodies were from BD Gentest (Worburn, MA) and rabbit anti-human CAR polyclonal antibodies were from CHEMICON (Temecula, CA). Rabbit anti-human GAPDH polyclonal antibodies were from IMGENEX (San Diego, CA). Alexa Fluor 680 donkey anti-goat IgG was from Invitrogen. IRDye 680 goat anti-rabbit IgG was from LI-COR Biosciences (Lincoln, NE). All other chemicals and solvents were of the highest grade commercially available.

*Human livers and cell culture conditions* - Human liver samples from 25 donors were obtained from Human and Animal Bridging (HAB) Research Organization (Chiba, Japan). The human hepatocellular carcinoma cell lines HepG2 and HuH7 were obtained from Riken Gene Bank (Tsukuba, Japan), and HLE was from Japanese Collection of Research Bioresources (Tokyo, Japan). The human colon carcinoma cell lines LS180 and Caco-2, the human embryonic kidney cell line HEK293, and the human breast adenocarcinoma cell line MCF-7 were obtained from American Type Culture Collection (Rockville, MD). HepG2, HuH7, and HLE cells were cultured in Dulbecco's modified Eagle's medium (DMEM) (Nissui Pharmaceutical, Tokyo, Japan) supplemented with 10% fetal bovine serum (FBS) (Invitrogen). LS180, Caco-2,

and MCF-7 cells were cultured in DMEM supplemented with 0.1 mM non-essential amino acid (Invitrogen) and 10% FBS. Differentiated Caco-2 (Caco-2/D) cells were obtained by culture for three weeks post-confluence. HEK293 cells were cultured in DMEM supplemented with 4.5 g/L glucose, 10 mM HEPES, and 10% FBS. These cells were maintained at 37°C under an atmosphere of 5% $CO_2$-95% air.

*Real-time RT-PCR for PXR and CYP3A4* - Total RNA was isolated from 25 human liver samples using ISOGEN (Nippon Gene, Tokyo, Japan) according to the manufacturer's protocol. The cDNAs were synthesized from total RNA using ReverTra Ace (Toyobo, Osaka, Japan). The forward and reverse primers for CYP3A4 were 5'-CCAAGCTATGCTCTTCACCG-3' and 5'-TCAGGCTCCACTTACGGTGC-3', respectively. The forward and reverse primers for human PXR were 5'-TGCGAGATCACCCGGAAGAC -3' and 5'-ATGGGAGAAGGTAGTGTCAAAGG -3', respectively. The real-time PCR was performed using the Smart Cycler (Cepheid, Sunnyvale, CA) with Smart Cycler software (Ver. 1.2b) as follows: after an initial denaturation at 95°C for 30 s, the amplification was performed by denaturation at 95°C for 6 s, annealing and extension at 68°C for 20 s for 40 cycles. The mRNA levels were normalized with GAPDH mRNA determined by real-time RT-PCR as described previously (19).

*SDS-PAGE and Western blot analyses of PXR and CYP3A4* - Whole cell lysates were prepared from 25 human liver samples by homogenization with lysis buffer (50 mM Tris-HCl (pH 8.0), 150 mM NaCl, 1 mM EDTA, 1% NP-40) containing protease inhibitors [0.5 mM APMSF, 2 μg/mL aprotinin, 2 μg/mL leupeptin]. The protein concentrations were determined using Bradford protein assay reagent (Bio-Rad, Hercules, CA) with γ-globulin as a standard. The whole cell lysates (10-50 μg) were separated with 7.5% SDS-polyacrylamide gel electrophoresis and transferred to Immobilon-P transfer membrane (Millipore, Bedford, MA). The membranes were probed with goat anti-human PXR, rabbit anti-human CYP3A4, goat anti-human HNF4α, rabbit anti-human CAR, or rabbit anti-human GAPDH antibodies and the corresponding fluorescent dye-conjugated second antibody, and the band densities were quantified with Odyssey Infrared Imaging system (LI-COR Biosciences). Nuclear extracts (10 μg) from the HepG2 and LS-180 cells were also used to determine the PXR protein level.

*Real-time RT-PCR for mature miR-148a* - For the quantification of mature miR-148a, polyadenylation and reverse transcription were performed using the NCode miRNA First-Strand cDNA Synthesis Kit (Invitrogen) according to the manufacturer's protocol. The forward primer for miR-148a was 5'-TCAGTGCACTACAGAACTTTGT -3', and the reverse primer was the supplemented universal qPCR primer. The PCR analyses were performed

as follows: after an initial denaturation at 95°C for 30 s, the amplification was performed by denaturation at 95°C for 10 s, annealing and extension at 64°C for 10 s for 40 cycles. The mature miR-148a level was normalized with U6 snRNA determined by real-time RT-PCR as described previously (20).

*Construction of reporter plasmids* - To construct luciferase reporter plasmids, various target fragments were inserted into the *Xba* I site downstream of the luciferase gene in the pGL3-promoter vector. The sequence from 3362 to 3383 in the human PXR mRNA (5'-ACAGACTCTTACGTGGAGAGTGCACTGA-3') was termed miR-148a recognition element (PXRMRE148). The fragment containing three copies of the PXRMRE148 (5'-CTAGAAGCCACAGACTCTTACGTGGAGAGTGCACTGACCTGTAGAAGCCACAGACTCTTACGTGGAGAGTGCACTGACCTGTAGAAGCCACAGACTCTTACGTGGAGAGTGCACTGACCTGTAT -3', PXRMRE148 is underlined) was cloned into the pGL3-promoter vector (pGL3p/3xPXRMRE). The complementary sequence of three copies of the PXRMRE148 was also cloned into the pGL3-promoter plasmid (pGL3p/3xPXRMRE-Rev). A fragment containing the perfect matching sequence with the mature miR-148a, 5'-CTAGACAAAGTTCTGTAGTGCACTGAT -3' (the matching sequence of miR-148a is underlined) was cloned into the pGL3-promoter vector (pGL3p/c-148a). The nucleotide sequences of the constructed plasmids were confirmed by DNA sequencing analyses.

*Luciferase assay* - Various luciferase reporter plasmids (pGL3p) were transiently transfected with pGL4.74-TK plasmid into HEK293 or HepG2 cells. Briefly, the day before transfection, the cells were seeded into 24-well plates. After 24 h, 70 ng of pGL3p plasmid, 30 ng of pGL4.74-TK plasmid and 4 pmol of the precursors for miR-148a or control were transfected into HEK293 cells using Lipofectamine 2000. For HepG2 cells, 80 ng of pGL3p plasmid, 20 ng of pGL4.74-TK plasmid and 10 pmol of the AsOs for miR-148a or control were transfected using Tfx-20 reagent. After incubation for 48 h, the cells were resuspended in passive lysis buffer, and then the luciferase activity was measured with a luminometer (Wallac, Turku, Finland) using the dual-luciferase reporter assay system.

*Transfection of precursor or antisense for miR-148a into HepG2 and LS-180 cells and isolation of nuclear extract and total RNA* - To investigate the effect of miR-148a on the expression of PXR protein, 50 nM precursor or 50 nM AsO for miR-148a or control were transfected into HepG2 cells using Lipofectamine RNAiMAX. After 72 h, total RNA was isolated using ISOGEN and the mature miR-148a levels were determined by Northern blotting as described above. Nuclear extract was isolated using the NE-PER Nuclear and Cytoplasmic extraction reagents (Pierce,

Rockford, IL) according to the manufacturer's protocol. LS180 cells were transfected with 50 nM precursor for miR-148a or control using Lipofectamine RNAiMAX. After 72 h, the cells were treated with 50 μM rifampicin or 0.1% (v/v) DMSO for 24 h. Then, total RNA and nuclear extract were isolated.

*Evaluation of the expression level of PXR in HepG2 using reporter construct containing PXR responsive element* - The reporter construct pCYP3A4-362-7.7K contains the promoter region (-362 to +11) including the ER6 (everted repeat separated by six nucleotides) motif and the distal enhancer region (-7836 to -7200) including the DR3 (direct repeat separated by three nucleotides) motif of the *CYP3A4* gene, to which PXR binds (21). The day before transfection, HepG2 cells were seeded into 24-well plates. After 24 h, 180 ng of pCYP3A4-362-7.7K, 20 ng of pGL4.74-TK plasmid and various doses of the precursors and AsOs for miR-148a or control were transfected using Tfx-20 reagent. After incubation for 48 h, the cells were treated with 10 μM rifampicin or 0.1% DMSO for 24 h, and then the luciferase activity was measured.

*Statistical analyses* - Statistical significance was determined by analysis of variance followed by Dunnett multiple comparisons test or Tukey method test. Comparison of two groups was made with an unpaired, two-tailed student's *t* test. Correlation analyses were performed by Spearman rank method. A value of $P < 0.05$ was considered statistically significant.

## RESULTS

*PXR protein level is not associated with PXR mRNA level in human livers* - We first examined the PXR mRNA level in a panel of 25 human livers by real-time RT-PCR assay and investigated the relationship with the PXR protein level. As shown in Fig. 1, no statistically significant correlation was observed between the PXR mRNA and protein levels (Rs = 0.10), indicating the involvement of post-transcriptional regulation of human PXR. To uncover the molecular mechanism of the post-transcriptional regulation, we sought to examine the involvement of miRNA-mediated regulation. Employing an on-line search using the miRBase Target database (15, http://microrna.sanger.ac.uk/), potential recognition elements for 16 kinds of miRNA such as miR-148a, miR-192, miR-560 were found in the 3' UTR in human PXR. Among them, we focused on miR-148a because it is selectively and abundantly expressed in liver (22) and has high complementarity in the 5' end at miRNA-mRNA duplexes including the seed sequence. The potential miR-148a target site is approximately 200 bases downstream of the stop codon of the human PXR mRNA. The alignment of hsa-miR-148a with the 3' UTR of human PXR mRNA (Fig. 2*A*) was drawn using RNAhybrid (23, http://bibiserv.techfak.uni-bielefeld.de/rnahybrid

/). We investigated whether this region termed the miR-148a recognition element (PXRMRE148) might be involved in the regulation of PXR by miR-148a.

*Expression levels of miR-148a in human cancer cell lines* – Real-time RT-PCR analysis using NCode miRNA First-Strand cDNA Synthesis Kit was performed to determine the expression levels of mature miR-148a in 8 kinds of human cancer cell lines (Fig. 2*B*). The mature miR-148a was detected in all cell lines tested in this study, with large variability among cell lines (37-fold). The U6 snRNA levels, which were used for normalization, varied < 3-fold in the experiment; much less than the miR-148a levels. The mature miR-148a was higher in HepG2 and differentiated Caco-2 cells than the other cell lines. It was also interesting that, in Caco-2 cells, the expression level of mature miR-148a was increased with differentiation. Thus, the expression levels of mature miR-148a were highly variable among the human cancer cell lines.

*Repressive regulation of PXR by miR-148a in human cell lines* - To investigate whether PXRMRE148 is functional in the regulation by miR-148a, luciferase assays were performed with HEK293 cells (Fig. 2*C*). We first confirmed that the luciferase activity of the pGL3p/c-148a plasmid, in which the miR-148a complementary sequence was inserted downstream of the *luciferase* gene, was significantly ($P < 0.01$) decreased by the co-transfection with the precursor for miR-148a. The luciferase activity of pGL3p/3xPXRMRE plasmid, in which three copies of the potential miR-148a recognition site were inserted downstream of the *luciferase* gene, was also significantly ($P < 0.01$) decreased by co-transfection with the precursor for miR-148a (33% of control), while that of pGL3p/3xPXRMRE-Rev plasmid with the inverted recognition site was not affected. In HepG2 cells, which showed the highest expression of miR-148a (Fig. 2*B*), the luciferase activities of pGL3p/c-148a and pGL3p/3xPXRMRE plasmid were significantly ($P < 0.01$) lower than those of the control pGL3p plasmid (Fig. 2*D*). These activities were significantly ($P < 0.01$) restored by the transfection of AsO for miR-148a. These results underscore that miR-148a functionally recognizes PXRMRE148 to decrease the expression.

*Effects of overexpression or inhibition of miR-148a on the PXR protein level in a human cell line* - We next examined the change in endogenous PXR protein expression by the overexpression or inhibition of miR-148a. By the transfection of the precursor for miR-148a into HepG2 cells that harbor the increased level of mature miR-148a, the PXR protein level was significantly ($P < 0.05$) decreased compared with the control (Fig. 3*A*). Conversely, by the transfection of the AsO for miR-148a into HepG2 cells, where the expression of mature miR-148a was extinguished, the PXR protein level was significantly ($P < 0.05$) increased

compared with the control (Fig. 3*B*). Meanwhile, the expression level of RXRα protein, a heterodimer partner of PXR, was not affected by the overexpression or inhibition of miR-148a. It is well known that ligand-activated PXR activates the transcription of targets by binding to the responsive element. Using the pCYP3A4-362-7.7K plasmid containing the PXR responsive element as a reporter construct, the changes in the PXR protein levels were monitored with the reporter activity (Fig. 3*C* and 3*D*). The luciferase activity of pCYP3A4-362-7.7K plasmid was prominently (5.3-fold) increased by the treatment with rifampicin in HepG2 cells (Fig. *3E*). Transfection of the precursor for miR-148a significantly decreased both the rifampicin-induced and basal transcriptional activities, resulting in a dose-dependent decrease of the induction. In contrast, the transfection of antisense for miR-148a significantly increased both the rifampicin-induced and basal transcriptional activity, resulting in a dose-dependent increase of the induction (Fig. 3*F*). These results suggest that miR-148a negatively regulates the expression of PXR protein and, subsequently, the induction of its targets.

*Role of miR-148a-dependent PXR regulation in the induction of endogenous CYP3A4 mRNA in a human cell line* - We next sought to examine whether the miR-148a-dependent change of the PXR protein level affects the CYP3A4 induction in human cells. LS-180 cells were used because this cell line expressed relatively higher CYP3A4 mRNA than the other cell lines (data not shown). By the transfection of the precursor for miR-148a into the LS-180 cells, the PXR protein level was significantly ($P < 0.01$) decreased (Fig. 4*A*), concomitant with dramatic increase of the mature miR-148a level, while the PXR mRNA level was not decreased at any time after the transfection (Fig. 4*B*). The RXRα protein level was not affected by the overexpression of miR-148a (Fig. 4*A*). As shown in Fig. 4*C*, the CYP3A4 mRNA level was significantly increased by the treatment with rifampicin (5.0-fold). However, this induction was diminished by the overexpression of miR-148a, although the basal CYP3A4 mRNA level was not affected. These results suggest that the miR-148a-dependent regulation of PXR affects the induction of CYP3A4.

*The miR-148a-dependent PXR regulation may control CYP3A4 expression in human liver tissue* - To further investigate the effects of the miR-148a-dependent regulation of PXR in human liver tissue, the relationships between the expression levels of miR-148a, PXR, and CYP3A4 were investigated using a panel of 25 human livers (Supplemental Table 1). The expression levels of miR-148a were variable (95-fold) in the panel of human livers. The miR-148a level in liver sample No. 18 was comparable to that in HepG2 cells. The PXR mRNA (75-fold) and CYP3A4 mRNA (363-fold) were also variable. As shown in Fig. 1, the PXR mRNA level was not correlated with

the PXR protein level. In contrast, the CYP3A4 mRNA level was significantly correlated (Rs = 0.67, $P < 0.001$) with the CYP3A4 protein level (Fig. 5*A*). When the PXR protein/PXR mRNA ratios were calculated as an index of the translational efficiency of PXR, they were inversely correlated with the miR-148a level (Rs = -0.41, $P < 0.05$, Fig. 5*B*), suggesting that PXR is negatively regulated by miR-148a in human liver. The PXR protein level was significantly correlated with both the CYP3A4 mRNA level (Rs = 0.47, $P < 0.05$, Fig. 5*C*) and the CYP3A4 protein level (Rs = 0.67, $P < 0.001$, Fig. 5*D*). As summarized in Fig. 5*E*, the post-transcriptional regulation of PXR by miR-148a appeared to have substantial impact on the CYP3A4 level in human livers.

## DISCUSSION

PXR regulates at least 40 genes encoding proteins responsible for the metabolism and elimination of drugs (14). The study of PXR regulation assists in the understanding of the inter- and intra-individual variability in the pharmacokinetics of drugs. Although many research groups have found variability in the PXR mRNA levels in human liver samples, the correlation with its protein level has not fully been investigated. In this study, we first demonstrated that there was no significant correlation between them in human livers. For human PXR, two splicing variants, including exon 1b (PXR.2) or deleting the 5'-end of the exon 5 (PXR.3), have been reported (24, 25), which cannot be distinguished with our PCR primers. However, since the expression levels of these splicing variants were extremely low in our analysis (data not shown), consistent with a report by Lamba et al. (26), the dissociation of the PXR protein level with its mRNA level is not an artificial phenomenon. Identification of the miRNA recognition element in the human *PXR* gene suggested the involvement of miRNA in the regulation of PXR.

The luciferase assays showed that the endogenous and exogenous miR-148a negatively regulated the activity through PXRMRE148. In addition, the endogenous PXR protein level was diminished by the overexpression of miR-148a and elevated by its inhibition. These results clearly indicated that human PXR is post-transcriptionally regulated by miR-148a. The miR-148a-dependent changes of PXR protein affected the induction of CYP3A4 in LS180 cells. To further investigate whether the miR-148a affects the induction of other targets of PXR, we determined the expression levels of MDR1 and CYP2B6 in LS180 cells (data not shown). Rifampicin induced the MDR1 (5-fold) and CYP2B6 (2-fold) mRNAs, known targets of PXR (27, 28), and the induction was attenuated by the overexpression of miR-148a. Thus, the miR-148a-dependent regulation of PXR appeared to affect its target genes in common.

Interestingly, the miR-148a recognition element is also present in the 3'-UTR of CYP3A4 mRNA. The complementarity of CYP3A4 with miR-148 (score 15.48, energy

-24.27) was higher than that of human PXR (score 15.14, energy -19.52). To investigate whether CYP3A4 is directly regulated by miR-148a, luciferase assays were performed using a plasmid containing three copies of the miR-148a recognition element in the *CYP3A4* gene. However, unlike the PXRMRE, the element in CYP3A4 did not respond to miR-148a (Supplemental figure 1), indicating that CYP3A4 is not directly regulated by miR-148a.

In the panel of human livers, the expression level of miR-148a was inversely correlated with the translational efficiency of PXR, supporting the role of miR-148a in the regulation of PXR in liver. The significant correlation between the CYP3A4 mRNA and the CYP3A4 protein level in human livers in this study, in accordance with previous studies (29, 30), supported the finding that miRNA did not directly regulate the CYP3A4 expression. The PXR protein level was correlated with the CYP3A4 mRNA level in human liver, indicating that miR-148a affects the CYP3A4 expression through modulating PXR expression. The PXR protein level was not correlated with the CYP2B6 (Rs = 0.31, $P > 0.1$) or MDR1 (Rs = -0.20, $P > 0.3$) mRNA levels in the panel of human livers (data not shown), in contrast to CYP3A4. Thus, we speculate that the PXR does not largely affect the constitutive expression of CYP2B6 and MDR1 in liver. In our panel of human livers, the CYP3A4 mRNA level was not correlated with the HNF4α protein level (Rs = -0.14, $P > 0.5$) or CAR protein level (Rs = 0.12, $P > 0.5$), indicating a significant contribution of PXR to the constitutive CYP3A4 level.

Most of the genes in the vertebrate nuclear receptor superfamily are strongly conserved between species. The ligand-binding domain of PXR shares amino acid identity of 75% between human and rodent, which can explain why the key ligands for PXR vary across species. Meanwhile, the DNA-binding domain of PXR shares more than 95% amino acid identity (1) inducing a similar set of genes. Most miRNAs are evolutionally conserved, which suggests that the miRNA-mediated regulation of certain genes would be common among species. The MRE148 is also identified in the 3' UTR in mouse PXR (score 16.63, energy -21.4) and rat PXR (score and energy are not calculated at miRBase, but has only a 1-base difference with the corresponding mouse sequence) at ~670-bp downstream of the stop codon, although the 3' UTR of PXR is poorly conserved between human and rodent. It is therefore possible that rodent PXR may also be regulated by miR-148a, suggesting that rodent might be a useful model animal to investigate the role of miR-148a in drug metabolism and elimination *in vivo*.

In conclusion, we found that human PXR is post-transcriptionally regulated by miR-148a affecting the CYP3A4 level in human liver. This study would provide new insight into the unsolved mechanism of the large interindividual variability of CYP3A4 expression.

*Acknowledgements*

We are grateful to Drs Kiyoshi Nagata and Yasushi Yamazoe (Division of Drug Metabolism and Molecular Toxicology, Graduate School of Pharmaceutical Sciences, Tohoku University, Sendai, Japan) for providing pCYP3A4-362-7.7K plasmid. We acknowledge Mr. Brent Bell for reviewing the manuscript.

## REFERENCES


1. Kliewer, S. A., Goodwin, B., Willson, T. M. (2002) *Endocr. Rev.* **23,** 687-702.
2. Meijerman, I., Beijnen, J. H., Schellens, J. H. (2006) *Oncologist* **11,** 742-52.
3. Staudinger, J. L., Goodwin, B., Jones, S. A., Hawkins-Brown, D., MacKenzie, K. I., LaTour, A., Liu, Y., Klaassen, C. D., Brown, K. K., Reinhard, J., Willson, T. M., Koller, B. H., Kliewer, S. A. (2001) *Proc. Natl. Acad. Sci. USA* **98,** 3369-74.
4. Xie, W., Radominska-Pandya, A., Shi, Y., Simon, C. M., Nelson, M. C., Ong, E. S., Waxman, D. J., Evans, R. M. (2001) *Proc. Natl. Acad. Sci. USA* **98,** 3375-80.
5. Blumberg, B., Sabbagh, W. Jr., Juguilon, H., Bolado, J. Jr., van, Meter, C. M., Ong, E. S., Evans, R. M. (1998) *Genes Dev.* **12,** 3195-205.
6. Lehmann, J. M., McKee, D. D., Watson, M. A., Willson, T. M., Moore, J. T., Kliewer, S. A. (1998) *J. Clin. Invest.* **102,** 1016-23.
7. Goodwin, B., Hodgson, E., Liddle, C. (1999) Mol. *Pharmacol.* **56,** 1329-39.
8. Ozdemir, V., Kalowa, W., Tang, B. K., Paterson, A. D., Walker, S. E., Endrenyi, L., Kashuba, A. D. (2000) *Pharmacogenetics* **10,** 373-88.
9. Lamba, J. K., Lin, Y. S., Thummel, K., Daly, A., Watkins, P. B., Strom, S., Zhang, J., Schuetz, E. G. (2002) *Pharmacogenetics* **12,** 121-32.
10. Floyd, M. D., Gervasini, G., Masica, A. L., Mayo, G., George, A. L. Jr., Bhat, K., Kim, R. B., Wilkinson, G. R. (2003) *Pharmacogenetics* **13,** 595-606.
11. Martínez-Jiménez, C. P., Jover, R., Donato, M. T., Castell, J. V., Gómez-Lechón, M. J. (2007) *Curr. Drug Metab.* **8,** 185-94.
12. Kretschmer, X. C., Baldwin, W. S. (2005) *Chem. Biol. Interact.* **155,** 111-28.
13. Pascussi, J. M., Drocourt, L., Fabre, J. M., Maurel, P., Vilarem, M. J. (2000) *Mol. Pharmacol.* **58,** 361-72.
14. Aouabdi, S., Gibson, G., Plant, N. (2006) *Drug Metab. Dispos.* **34,** 138-44.
15. Griffiths-Jones, S. (2004) *Nucleic Acids Res.* **32,** D109-11.
16. Bartel, D. P. (2004) *Cell* **116,** 281-97.
17. Lewis, B. P., Burge, C. B., Bartel, D. P. (2005) *Cell* **120,** 15-20.
18. Xie, X., Lu, J., Kulbokas, E. J., Golub, T. R., Mootha, V., Lindblad-Toh, K., Lander, E. S., Kellis, M. (2005) *Nature* **434,** 338-45.
19. Tsuchiya, Y., Nakajima, M., Kyo, S., Kanaya, T., Inoue, M., Yokoi, T. (2004) *Cancer Res.* **64,** 3119-25.
20. Tsuchiya, Y., Nakajima, M., Takagi, S., Taniya, T., Yokoi T. (2006) *Cancer Res.* **66,** 9090-8.

21. Takada, T., Ogino, M., Miyata, M., Shimada, M., Nagata, K., Yamazoe, Y. (2004) *Drug Metab. Pharmacokinet.* **19,** 103-13.

22. Barad, O., Meiri, E., Avniel, A., Aharonov, R., Barzilai, A., Bentwich, I., Einav, U., Gilad, S., Hurban, P., Karov, Y., Lobenhofer, E. K., Sharon, E., Shiboleth, Y. M., Shtutman, M., Bentwich, Z., Einat, P. (2004) *Genome Res.* **14,** 2486-94.

23. Rehmsmeier, M., Steffen, P., Hochsmann, M., Giegerich, R. (2004) *RNA* **10,** 1507-17.

24. Bertilsson, G., Heidrich, J., Svensson, K., Asman, M., Jendeberg, L., Sydow-Bäckman, M., Ohlsson, R., Postlind, H., Blomquist, P., Berkenstam, A. (1998) *Proc. Natl. Acad. Sci. USA* **95,** 12208-13.

25. Dotzlaw, H., Leygue, E., Watson, P., Murphy, L. C. (1999) *Clin. Cancer Res.* **5,** 2103-7.

26. Lamba, V., Yasuda, K., Lamba, J. K., Assem, M., Davila, J., Strom, S., Schuetz, E. G. (2004) *Toxicol. Appl. Pharmacol.* **199,** 251-65.

27. Synold, T. W., Dussault, I., Forman, B. M. (2001) *Nat. Med.* **7,** 584-90.

28. Goodwin, B., Moore, L. B., Stoltz, C. M., McKee, D. D., Kliewer, S. A. (2001) *Mol. Pharmacol.* **60,** 427-31.

29. Westlind-Johnsson, A., Malmebo, S., Johansson, A., Otter, C., Andersson, T. B., Johansson, I., Edwards, R. J., Boobis, A. R., Ingelman-Sundberg, M. (2003) *Drug Metab. Dispos.* **31,** 755-61.

30. Watanabe, M., Kumai, T., Matsumoto, N., Tanaka, M., Suzuki, S., Satoh, T., Kobayashi, S. (2004) *J. Pharmacol. Sci.* **94,** 459-62.